

PATs selection towards sustainability in irrigation networks: Simulated annealing as a water management tool



Modesto Pérez-Sánchez ^a, Francisco Javier Sánchez-Romero ^b, P. Amparo López-Jiménez ^a, Helena M. Ramos ^{c,*}

^a Hydraulic and Environmental Engineering Department, Universitat Politècnica de Valencia, Valencia, 46022, Spain

^b Rural and Agrifood Engineering Department, Universitat Politècnica de València, Valencia, 46022, Spain

^c Civil Engineering, Architecture and Georesources Department, CERIS, Instituto Superior Técnico, Universidade de Lisboa, Lisboa, 1049-001, Portugal

ARTICLE INFO

Article history:

Received 10 September 2016

Received in revised form

1 September 2017

Accepted 16 September 2017

Available online 17 September 2017

Keywords:

PAT

Energy recovery

Irrigation networks

Simulated annealing

ABSTRACT

Irrigation networks involve many water and energy aspects, in which the sustainability plays a paramount role. Nowadays, water tariff in irrigation networks represents a high percentage within of farmers' costs, partially due to the low hydraulic and energy efficiency. The installation of pumps working as turbines enables to reduce the pressure and it makes possible the energy generation. In this research, a new maximization methodology to recover energy, considering the feasibility of the installation, was proposed to allocate PATs within networks. Simulated annealing techniques were used with different objective functions as well as different number of machines. Once the maximum energy lines were defined, real machines were selected through the discharge and the head number, considering the available net head in each allocation. Furthermore, the use of WaterGEMS® software enabled to simulate the flow, the pressure and the efficiency variation in the installed machine over time. The combined use of WaterGEMS® and the simulated annealing in the proposed methodology is a powerful water management tool towards the search of the sustainability in irrigation networks. To illustrate the proposed methodology, a case study was presented, obtaining a recovered energy of 26.51 MW h/year (10% of the provided energy in the network).

© 2017 Elsevier Ltd. All rights reserved.

1. Introduction

Nowadays, the development of the current society is conditioned by the use and the implementation of renewable energies. This expansion is established by European Union's policy, which has the objective of reducing the greenhouse gas emissions down to 20% [25]. Therefore, considering the consumption in water pressurized systems that represents approximately 2–3% of the worldwide energy consumption [35], the use of hydropower plants in these infrastructures becomes of paramount relevance [42] to make possible the energy recovery and as a consequence, the implementation of these actions contributes to improve the water management, increasing the sustainability (*i.e.*, reduction of leakage and pipe breaks, as well as the generation of renewable

energy for sale or personal consumption) [7,10].

The energy recovery in water supply systems has been studied by different authors in terms of replacing pressure reduction valves (PRVs) by mini-hydropower stations [9], with suitable pump working as turbines (PATs) [10,11,42], and maximizing the use of the theoretical energy available [47,48]. These studies were focused on drinking systems which are different to irrigation networks because in the latter, the demand is more variable and it is function of agronomic parameters, being more difficult to determine the consumption patterns [38]. However, other different hydraulic machines can be used. Different authors proposed some other prototypes such as the vertical-axis turbine [14]. Similar prototypes, patented by Politecnico di Milano, were analyzed and tested by Refs. [27,28]; in order to know the behaviour of its hydraulic characteristics and recovery power in two different vertical-axis turbines, which have three and five blades, respectively [17]. developed an optimization proposal considering Kaplan and Francis turbines. In this line [42], and later, [47] [48]; proposed and

* Corresponding author.

E-mail addresses: mopesan1@upv.es (M. Pérez-Sánchez), fcosanro@agf.upv.es (F.J. Sánchez-Romero), hramos.ist@gmail.com (H.M. Ramos).

developed experimentally a tubular propeller turbine. This machine was tested in the laboratory and its curves were used to optimize one case study in Lausanne (Switzerland).

In pressurized irrigation networks, different researchers analyzed the optimization of the energy consumption in pumped systems [22,32,36]; while others developed strategies to perform energetic audits in irrigation pressurized systems [1,7,36,45]. However, the analysis of the potential recovered energy has not been performed deeply yet. Regarding this topic, preliminary studies were only made. Some of these studies considered the average flows [19] and others researches analyzed the discretized flows and calculated the theoretical recovered energy in some pipe branches of a network (*i.e.*, in line, in hydrant or in irrigation point) [37].

The present research promotes the study of energy recovery considering several factors, such as the farmers' demands which depend on different habits (*i.e.*, irrigation endowment, maximum days between irrigations, weekly trend of irrigation, and irrigation duration); the location of the turbines which maximizes the theoretical recovered energy as a function of the number of turbines; the selection of the hydraulic machine to be installed on the recovery point (*i.e.*, specific speed, diameter of the impeller, rotational speed); and the analysis of recovered energy as a function of performance of the machine.

Different authors have proposed different strategies more or less complexes for placing the machines. These strategies are focused on maximizing the recovered energy or minimizing the excess of the pressure [20,47]; although the localization of these places is not perfectly defined yet. In similar problems, stochastic methods were used for PRVs implementation [2]; sizing the diameter of pipes in networks [26,44,51]; minimizing the use of energy in pumped networks [39], among others. The impossibility to reach the optimal solution as a consequence of the complexity of real scenarios and the highly combinatorial nature of them induced the development of new solution procedures. These methodologies are based on metaheuristic algorithms [53] such as simulated annealing [47], tabu search [16] or particle swarm optimization [4,5,6,23].

The main contribution of this research is a new methodology based on an objective function with a feasibility index to allocate turbines in water pressurized networks, considering the simulated annealing to get the best solution approach in this water management problem. This methodology was applied to a case study, in which the turbines machines were defined by non-dimensional curves. The case study was simulated with WaterGEMS® software [34] to obtain the recovered energy. WaterGEMS is a private domain software that provides a decision support tool for water distribution networks improving the operational knowledge of the hydraulic system. This software can represent different elements (*e.g.*, pipes, joints, pumps, turbines, valves) as well as optimization strategies to minimize the consumed energy in pump systems or determining pipe sizes as a function of the investment cost, circulating flows and restriction of pressure by means the use of the genetic algorithm.

2. Material and methods

2.1. Analysis of recovered energy

In this section, the mathematical analysis to recover energy is performed when there are installed turbines in series which can be installed in all pipes (Fig. 1) since there is available energy.

If a turbine is installed in the pipe system, the recovered energy is determined by equation (1):

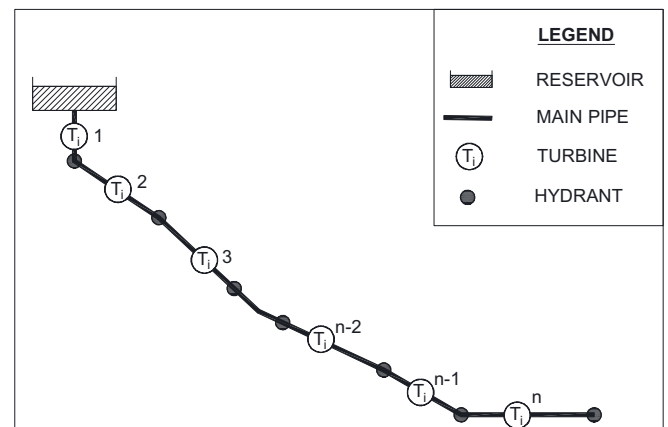


Fig. 1. Pipe system with “n” turbines installed in series in all lines.

$$E_{R_i}(\text{kWh}) = \sum_{k=1}^{k=p} \eta \gamma Q_{ik} (p_{ik} - \max(p_{min_i}; p_{min_l})) \Delta t \\ = \sum_{k=1}^{k=p} \eta \gamma Q_{ik} H_{ik} \Delta t \quad (1)$$

where E_{R_i} is the recovered energy in line 'i' (kWh); 'R', means the energy recovery value is obtained with a defined machine; i is the line of the system where the turbine is installed, which varies between 1 and 'n'; k is the time interval analyzed which varies between 1 and 'p'; p is the number of analyzed intervals; η is the efficiency of the machine; γ is the specific weight of the fluid (N/m^3); p_{ik} is the service pressure in any point of the network in the interval k (m w.c.); Q_{ik} is the circulating flow by a line i , in the interval k ; H_{ik} is the value of the head in irrigation point, hydrant or line, in the interval k (m w.c.); p_{min_i} is the minimum pressure of the line or hydrant to ensure the minimum pressure in the most disadvantageous consumption node (m w.c.); p_{min_l} is the minimum required pressure of an irrigation point to ensure the evenly irrigation water (m w.c.); H_i is the head value in the irrigation point, hydrant or line (m w.c.); Δt is the time interval (s).

When several turbines are installed, the recovered energy in each line is equal to equation (2):

$$E_{Ri}^s = \sum_{k=1}^{k=p} \eta \gamma Q_{ik} \left(H_{ik} - \sum_{i=1}^{i=m} (H_{ik}^s) \right) \Delta t \quad (2)$$

where m is the number of installed turbines upstream which varies between 0 and 'n-1'; n is the total number of installed machine in the water network; E_{Ri}^s is the recovered energy by the turbine that is installed in the line 'i' with other turbines installed in series (kWh); H_i^s is the recovered head by other installed turbines in series which are installed upstream to line 'i' (m w.c.).

For example, if the pipe system has three lines ($n = 3$), the recovered energy, according to equation (2) is:

In line 1 ($i = 1$),

$$E_{R1}^s = \sum_{k=1}^{k=p} \eta \gamma Q_{1k} (H_{1k}) \Delta t;$$

In line 2 ($i = 2$),

$$E_{R2}^s = \sum_{k=1}^{k=p} \eta \gamma Q_{2k} (H_{2k} - H_{1k}) \Delta t;$$

In line 3 ($i = 3$),

$$E_{R3}^s = \sum_{k=1}^{k=p} \eta \gamma Q_{3k} (H_{3k} - H_{2k}) \Delta t;$$

Therefore, the total recovered energy with installed turbines in series (E_{TR}^s) is $E_{R1}^s + E_{R2}^s + E_{R3}^s$. For 'n' turbines in series in 'n' lines, the E_T^s is defined by equation (3):

$$E_{TR}^s = \sum_{i=1}^{i=n} E_{Ri}^s \quad (3)$$

If the E_{TR}^s analysis is performed in a branched network (Fig. 2), E_{TR}^s is defined by equation (4):

$$E_{TR}^s = \text{tr}[[A][B][C]] = \text{tr}[D] \quad (4)$$

where E_{TR}^s is the total theoretical recovered energy in the network (kWh); [A] is the matrix (nxn) made up zero or one. The matrix has 'n' rows, where 'n' is the number of turbines and 'i' columns, being 'i' the number of lines of the network. This matrix defines where the turbines are installed. If the value is one, the turbine is installed in this line, otherwise, the line 'i' doesn't have installed turbine; [B] is the matrix (ixi) which defines the recovered energy in the line, when another turbine upstream exists. This matrix is constant in the network and it is defined by the number of lines of the network (i). [C] is the matrix (nxn) and its value is 0 or 1 which defines the lines where the turbines are placed upstream. This matrix is generated according to the topology of the network and the matrix can only present one or zero in each element; [D] is the matrix (nxn) which is the product of the previous matrixes ([A][B][C]). When this product is calculated and the matrix trace ((tr) [D]) is determined, the obtained value is the theoretical recovered energy in the network (E_{TR}^s). The trace is the value that is obtained by the addition of all the elements of the main diagonal of a squared matrix.

2.2. Optimization methodology for maximizing energy

Simulated annealing (SA) is a search heuristic algorithm which is based on the analogy with the physics process of annealing of metals. The algorithm is inspired in Monte-Carlo's method [24], based on Metropolis's idea [31] applied it to the optimization of combination problems. This method is a powerful tool for both discrete as continuous problems [51] and can robustly find the best solution in different problem typologies, where a high number of combinations occurs, according to the defined objective function

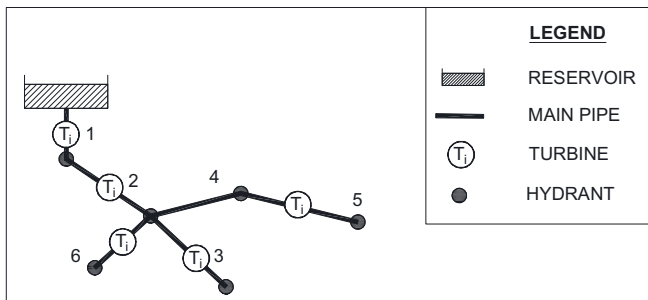


Fig. 2. Branched network with "n" turbines installed.

[46,52,55].

Hence, the maximization problem (Fig. 3) is defined:

1. Definition of the objective function (Ψ_i). Two different functions were studied to analyze the maximization of the recovered energy in the network by equations (5) and (6):

$$\Psi_1 = E_{TR}^s \quad (5)$$

$$\Psi_2 = \frac{E_{TR}^s}{PSR} = \frac{\Psi_1}{PSR} \quad (6)$$

where PSR is the period simple return which is lately defined in Section 2.5. When equation (6) is used the considered averaged performance is 0.55 according to the author [13]. This objective equation (Ψ_2) considers both the recovered energy and feasibility of the recovery system before selecting the line to install the turbine group. On the one side, energy is considered across (Ψ_1) defined in equation (5); on the other side, economical aspects are considered by PSR concept. Consequently, the investment and performance are both considered in the optimization process.

2. A list of the lines in descendent order is developed, according to the analyzed objective function. When equation (5) is used, the

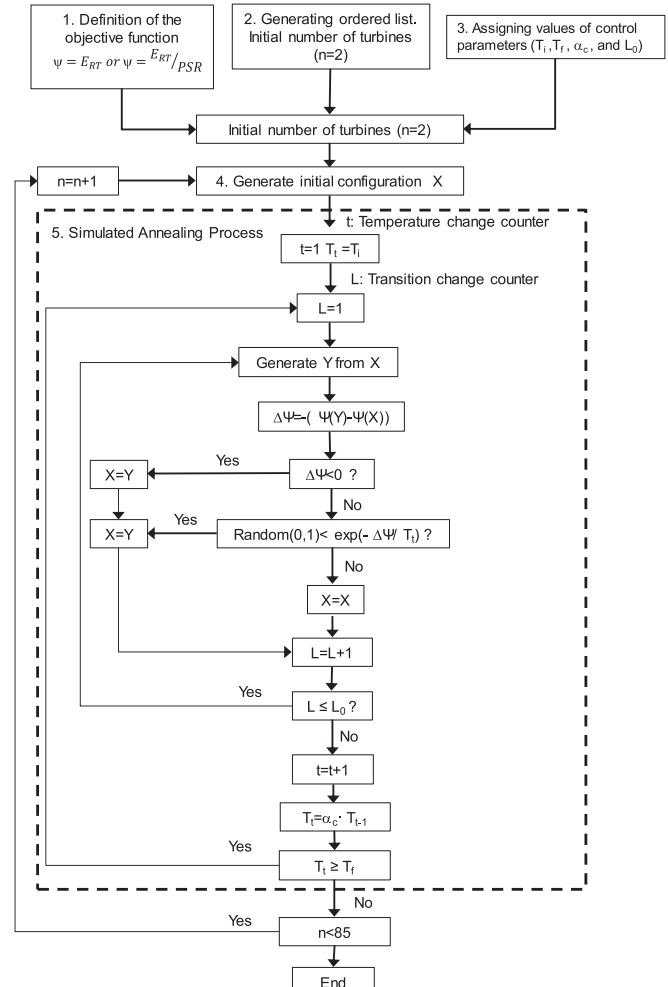


Fig. 3. Flowchart for networks optimization in the energy recovery process with "n" installed turbines.

- order is established according to the theoretical energy recovery in a line (E_{Ti})
3. The values of the control parameters are assigned to characterize the simulated annealing process, defining the number of iterations. These parameters are the initial temperature (T_i), the final temperature (T_f), the cooling rate (α_c) and the number of transitions (L_0) in each temperature step (T_t). These parameters are fixed according to a sensitivity analysis previously performed and they are changed depending on the objective maximized function which were attached in Results section.
 4. The initial combination (X), $X = (x_1, x_2, \dots, x_n)$, is established, in which ' n ' is the number of turbines and ' x_i ' is the line where each turbine is located: when n is 2, the selected lines are the first two lines. If the initial combination is n upper than 2, the process starts with the obtained solution for ' $n-1$ ' turbines. The line with the greater value of the objective function is added to this initial result that is not contained in the solution. This line is taken to the ordered list.
 5. The development of the simulated annealing process, in which a new combination (Y) is generated according to the general process that was described by Ref. [51]. For each iteration, a line is randomly deleted of the combination, and other line is randomly introduced. This addition is carried out considering the lines with better position in the ordered list (Step 2) with higher probability to be introduced in the new combination $Y = (y_1, y_2, \dots, y_n)$.

2.3. PATs selection

The selection of the hydraulic machines is very important in the procedure of energy recovery, considering that the water manager has to guarantee the quality service to users, and therefore, ensuring the established minimum pressure (normally, in irrigation networks, this pressure is equal to 30 m w.c. in the consumption node).

Hence, the use of *PATs* in non-conventional heads was analyzed by numerous authors with variable flows and heads. These authors proposed the use of recovery systems at remote areas [3,40]; as well as the development of the small applications in water pressurized systems, which are mainly allocated on drinking systems [9,10,11,12,21,25,41,42,47,48]; or irrigation [19,37]. The suitability for using these machines is due to: the wide range of pumps existing in the market, the low price, and the high availability when *PATs* are compared with the conventional turbines [41].

Different authors [18,30,43,50,54] analyzed the characteristic curves 'Q-H' and efficiency variation based on the non-dimensional parameters of the hydraulic machines, such as the discharge number (ϕ) and the head number (ψ). These parameters are defined by equations (7) and (8):

$$\phi = \frac{Q}{ND^3} \quad (7)$$

$$\psi = \frac{gH}{N^2 D^2} \quad (8)$$

Fig. 4 shows the values of the head number and the efficiency (η) for turbines with different values of the specific speed (ss) as a function of the discharge number. The specific speed is defined by equation (9):

$$ss = N \frac{\sqrt{P_R}}{H_R^{1.25}} \quad (9)$$

where N is the rated rotational speed (rpm); P_R is the rated power

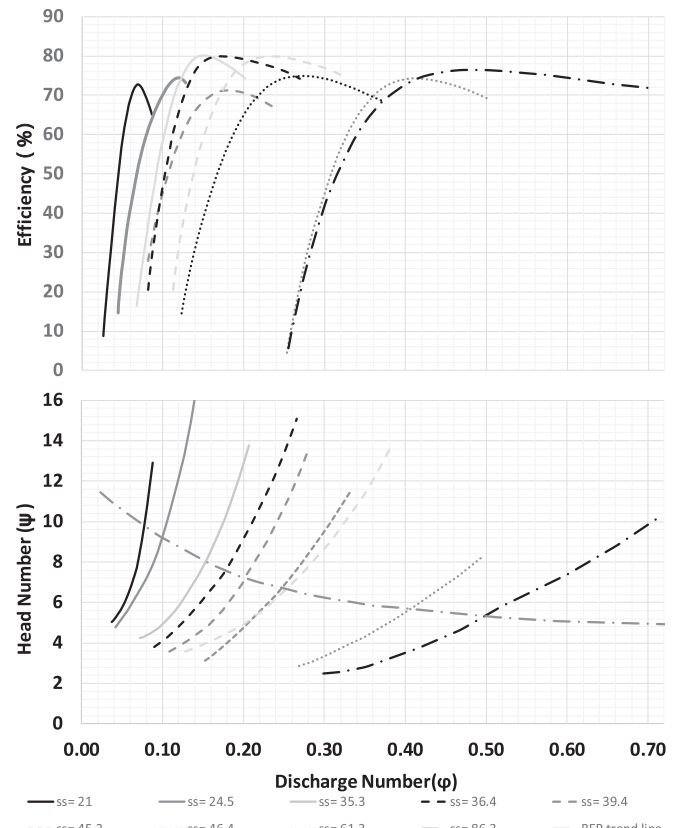


Fig. 4. Head number and efficiency depending on the discharge number (adapted from Ref. [43,50]).

(kW); H_R is the rated head (m w.c.); being 'R' the turbine design point or the best efficiency condition.

Fig. 4 also confirms the high variation of the efficiency when the turbinated flow varies. Still, in this figure, the best efficiency point (BEP) trend line is represented, enabling the visualization of the BEP as a function of the specific speed of the machine.

The assignation of the flow values and the available net head (H_T) in each line were obtained by using the methodology proposed by Ref. [37]. These flows were determined based on open probability of each irrigation point according to farmers' habits. Then, the energy balance determined the operation zone of the recovery systems. This operation zone must ensure the pressure for all users in all operating range and the selected machine cannot absorb more head than H_T . This premise must always be considered and it prevails on the energy recovery because the water distribution networks can be multipurpose systems, but the power generation is not the first objective of the networks [15].

Fig. 5 shows the criterion to select the operation range of the hydraulic machine. The diameter of impeller (D) and the rotational speed (N) were fixed considering the available net head. To select the upper flow limit in the operation range of the recovery system, the arbitrary adopted criterion was to ensure the energy recovery until 80% of the cumulative flow frequency at least in the studied line. This criterion was defined considering the high variability of the PAT performance, when the flow varies. Particularly, in these networks, the flow variability is very high over time. In order to increase the operation range, the installation of parallel machine group was considered. The number of installed machines will depend on their characteristic curve and the rotational speed.

Fig. 6 shows the proposed scheme to install the recovery system in each line. This scheme includes: one flowmeter, for measuring

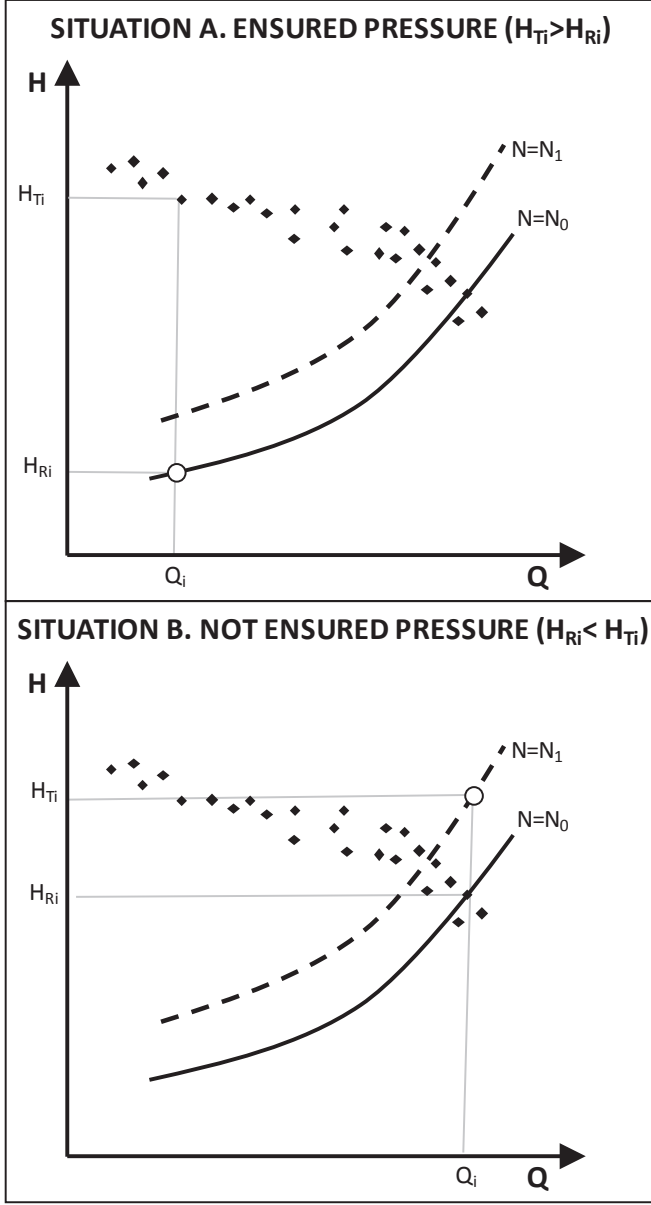


Fig. 5. Criterion to select the machine for the flow range in the irrigation points. (A) Ensured and (B) Not ensured pressure.

the instantaneous flows; isolation valves (IV), installed upstream to each PAT (their number is equal to the number of parallel PATs installed. Besides, one additional valve was considered to make possible the by-pass when the system doesn't generate energy for PAT maintenance); and PATs number varies as a function of the characteristic curve to reach 80% at least of the cumulative flow frequency in each line.

The operation mode is then described below and this is shown in Fig. 7. When a particular "k" hour is analyzed, if the estimated flow is between the minimum flow in line ($Q_{\min \text{ in line}}$) and the minimum operation flow, defined for one PAT ($Q_{\min \text{ 1PAT}}$), the isolation valve 4 (IV4) is open, and the remaining valves (IV1, IV2, and IV3) are closed. If the instant flow is between $Q_{\min \text{ 1PAT}}$ and the maximum operation flow, defined for one PAT ($Q_{\max \text{ 1PAT}}$), IV1 is open and the remaining valves are closed. When the flow increases until $Q_{\max \text{ 1PAT}}$, the second PAT must be connected and the IV2 changes its state from closed to open. This position is maintained in

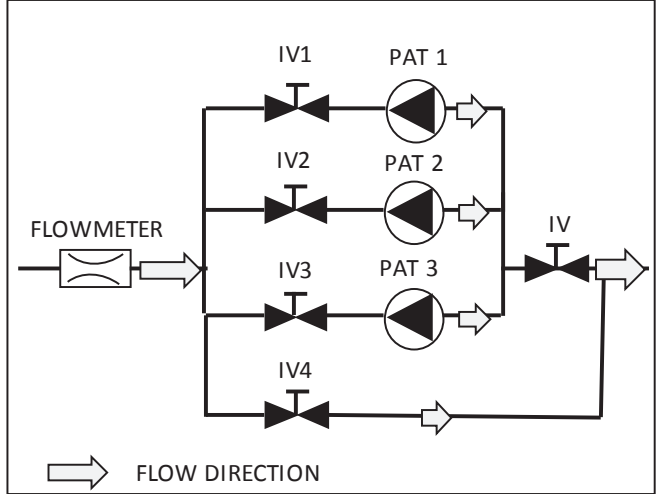


Fig. 6. Scheme proposed for installing the PATs in parallel.

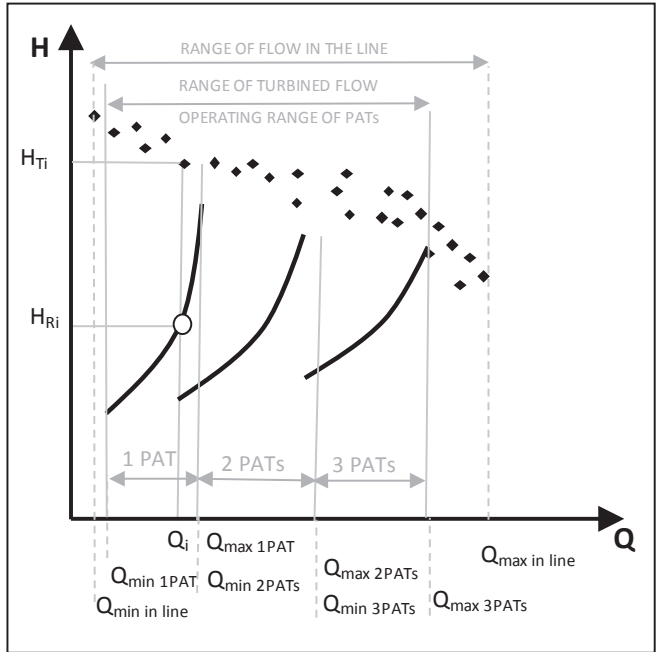


Fig. 7. Scheme for the operation zone.

the flow range. The lower limit is the minimum operation flow that is defined for two installed PATs in parallel ($Q_{\min \text{ 2PAT}}$; $Q_{\min \text{ 2PAT}} = Q_{\max \text{ 1PAT}}$) and the upper limit is the maximum operation flow which is defined for two installed PAT in parallel ($Q_{\max \text{ 2PAT}}$). This situation is recurrent as a function of the number of installed PATs. When the flow is higher than the maximum operation defined flow ($Q_{\max \text{ 3PAT}}$), the isolation valve of the bypass (IV4) is open and the other valves are closed when the flow range is between the maximum operation flow for "n" installed PATs (in Fig. 7., the number of machines is equal to three (n = 3)) and the maximum circulating flow ($Q_{\max \text{ in line}}$).

2.4. Analysis of recovered energy

Once operation curves have been defined for the selected lines of the network, in which the machines were allocated according to

the established solution in the optimization procedure, the next step was the maximization of the recovered energy. To do so, the network was modelled by using WaterGEMS for an extended period simulation. The simulation was performed according to different constraints: the demand's patterns of all consumption points, the PATs operation scheme previously described, and the operation curves of energy recovery.

Subsequently, the obtained flow and recovered head results were processed and the efficiency was determined over time in each machine. This analysis enabled to know the recovered energy (E_R); the recovery coefficient (RC) that was defined as the ratio between recovered energy and the theoretical energy (E_T) in the line; the maximum power installed (P_{max}), which corresponds to the maximum generated power by the machine; the minimum installed power (P_{min}) that is referred to the minimum performed power by the machine; the maximum efficiency (η_{max}), the minimum efficiency (η_{min}) and the average weighted efficiency (η_w) that is developed by the machine over time; the operation time of each machine (t_{nT}); the total recovered energy (E_{TR}) in the network (when the total number of the installed turbines (n) in the parallel group is considered in all lines); and the total recovery coefficient (TRC) in the network.

2.5. Maximum number of turbines to be installed

The installation of a high number of turbines implies a greater recovered energy. However, the maximum number of installed turbines in a branched network should be established considering the recovered energy as well as the economic feasibility. Although several authors used different economic criteria to define the feasibility of the recovery system (e.g., [13,56]), proposing the following indicators:

a) Period simple return (PSR). This indicator is defined by equation (10):

$$PSR = \frac{IC}{I - C} \quad (10)$$

where IC is the investment cost (€) [10], estimated this value in 545 €/kW (it is an average value considering the turbines group and its installation (i.e., civil, electrical and electronic equipment) when the pump working as turbine is used for installed power below to 10 kW; I is the annual income (€/year); and C is the annual operating cost (€/year).

The annual income (I) is defined by equation (11):

$$I = P_E E_{TR} \quad (11)$$

where P_E is the selling energy price (€/kWh); E_{TR} is the recovered energy that is obtained throughout simulation by using WaterGEMS®. When the hydropower station injects the energy on the grid, P_E is the sale price of the energy. If the hydropower station is used for self-consumption, P_E is the purchase price of the electric energy for the consumer. In this case, the average considered price is 0.0842 €/kWh.

The annual operation cost (C) is defined by equation (12):

$$C = C_0 E_{TR} \quad (12)$$

where C_0 is the unit operation cost (€/kWh) [13], estimated this parameter as 0.0145 €/kW; b) Energy index (EI) which is the ratio between IC and E_{TR} and this index is defined by equation (13):

$$EI = \frac{IC}{E_{TR}} \quad (13)$$

According to [13]; these installations are viable whether PSR is lower than six years and the energy index is smaller than 0.6 €/kWh.

3. Cases study

The application of this methodology was carried out in two different scenarios. Firstly, the proposed methodology was applied in a synthetic network (Case study 1) to check the success of the described methodology. In this virtual network, the obtained values of the recovered energy applying the proposal methodology were compared to the obtained values through analysis of all possible combinations (considering any position of turbines in any line). Once, the methodology verified, it was applied in a second scenario (Case study 2) that was located on Vallada (Valencia, Spain).

3.1. Case study 1. Description of the synthetic network

A synthetic network was developed to analyze the robustness of the proposed methodology (Fig. 8.). The branched network had twenty lines, twenty hydrants and eighty consumption points. The total assigned demand in each irrigation point was 1 l/s and four different kind of consumption nodes were defined as a function of the number of sectors (i.e., 1, 2, 3 or 4 sectors). Each type of irrigation point had a different area (i.e., sector-1 area was 0.27 ha, sector 2-area was 0.54 ha, sector 3-area was 0.81 ha, and sector 4 area was 1.08 ha) and its irrigation amount was 3.7 l/s·ha.

The assigned irrigation needs were applied on all consumption nodes and the considered crop was citrus, being the annual irrigation needs equal to 5736 m³/year. To determine the flow over time in each line, the proposed methodology of [37] was applied, considering an irrigation trend pattern equal to 1. The maximum days between irrigation was 1 and the daily probability was the same along the day.

3.2. Case study 2. Description of the irrigation network

In order to apply the described methodology to determine the optimal number of turbines to be installed in a water network, a real case study that corresponded an irrigation network was here described.

The modelled network was located in Vallada (Spain), the irrigated area was 290.2 ha and the main irrigated crop was citrus. The irrigation system (Fig. 9) was designed as an on-demand branched network (the users always get the water resource with enough quality and quantity). The difference of topographic elevation between the higher and the lower irrigation point was 130 m and the high reservoir ensured the minimum pressure of 30 m w.c. in all consumption points. The diameter of pipelines varied between 150 and 500 mm and they were of different materials (i.e., asbestos cement, polyvinyl-chloride and ductile iron). The total number of hydrants was seventy, and the total irrigation points were 371. These consumption points were connected with the hydrants by polyethylene pipelines.

3.3. Assumptions

Although the maximization of the number of turbines to install in this network could be to eighty-five, the maximum number of the modelled lines was four, when the feasibility criterion was

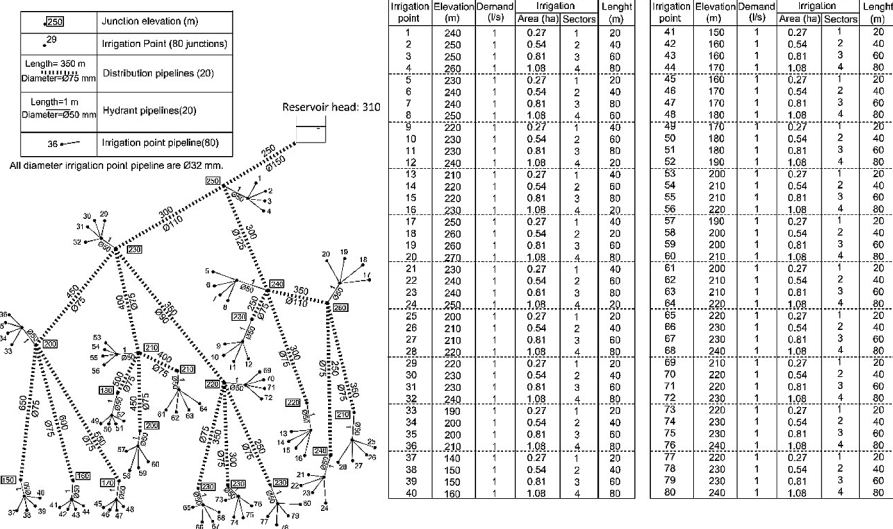


Fig. 8. Case study 1. Synthetic network.

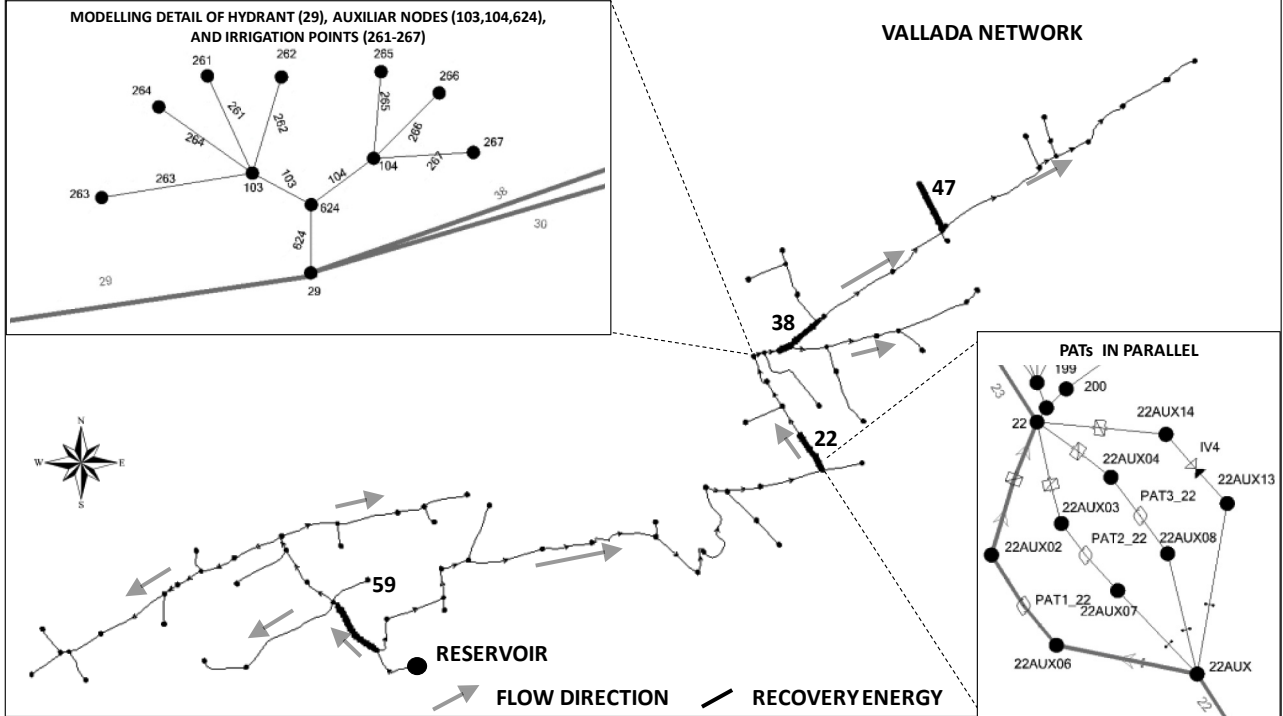


Fig. 9. Case study 2. Vallada (Spain).

considered. However, when the recovery analysis was done using WaterGEMS®, four realistic assumption were adopted since the consideration of a high number of turbines in the network doesn't have feasibility and currently, it can complicate the management of the network in terms of regulation of machine both parallel and in series. If the previous analysis determines more cases are necessary, new assumptions will be defined and they will be included in the model. In this case, the modelled assumptions were:

- Assumption A: Only one parallel group of turbines was installed in the network. According to the obtained results in the theoretical maximization, the line with greater E_T was

selected. In this case, one group of turbines is installed in the developed model in WaterGEMS, in which, the turbines and their operation were defined in Section 2.3. The scheme of the model to simulate the PAT group is shown in Fig. 9.

- Assumption B: Two lines with installed turbines were modelled in the network; these lines corresponded to the theoretical combination in which the recovery energy was maximum. For the assumption B, two group of turbines were inserted in the model, according to the results of the optimization. The PAT were selected according to the described criteria in Section 2.3, being the different PATs.

- c) Assumption C: Following the same criterion of a) and b), the model is run with three different groups of turbines using the solution obtained on the optimization process.
- d) Assumption D: In the last assumption, four PAT groups were simulated in the model. To characterize it, the model uses the solution of the simulated annealing, maximizing the recovered energy and considering the four lines where the energy recovery is higher.

4. Results and discussion

4.1. Case study 1. synthetic network

Tables 1 and 2 show the obtained results in the synthetic network when the proposed methodology was applied. To analyze the robustness of this proposed process, for each objective function, the best optimized result was compared with the higher value that was determined by calculating all possible combinations. To develop the optimization when the synthetic network was optimized considering the first objective function (Ψ_1), the initial temperature (T_i) was 100, the final temperature (T_f) was 0.01, the colling rate (α) was 0.9, the number of transitions was 10, and the number of iterations was 792 for each optimization process according to the number of installed turbines. When the second function (Ψ_2) was optimized, the initial temperature was 10, the final temperature was 0.01, the colling rate was 0.9, the number of transitions was 10 and the total number of the iterations was 594. The proposed methodology determined 7128 iterations to estimate the optimized solution, taking 17 min. All possible combinations were determined by 616645 iterations and the time was 1500 min

approximately.

Table 1 shows the optimization procedure when Ψ_1 is analyzed. For this example, the optimization obtained the best solution in all considered cases from two to ten turbines. Therefore, the difference between the values for recovered energy was zero, getting the best solution within the first hundred iterations. A number of iterations was only higher (361, **Table 1**) when nine turbines were optimized. When **Table 2** is consulted, the results were also suitable. The maximum difference of the obtained values by using simulated annealing was 1.01% when ten machines were considered. Both tables show the methodology got optimized solutions when they were compared with the obtained values, which were determined calculating all possible combinations, for each objective function.

4.2. Case study 2. irrigation network

4.2.1. Model developed for flow estimation

Before allocating the recovery machines, flows were estimated for any line of the network and they were compared to the available measurements. The calibration of the model presented a Nash-Sutcliffe index upper to 0.40, root relative squared mean error below 0.7 and percent bias below 5% [37] as calibration parameters. As a consequence, the model calibration is considered “good” according to [8] and [33] and these values didn’t present significative variability when the simulation was repeated. Hence, once the model was calibrated, the flows were used to maximize the objective functions and to analyze the selected turbines, which are modelled in WaterGEMS®.

The developed model (**Fig. 9**) had 647 lines, of which, 85 lines connected the branched network, 341 lines corresponded to

Table 1
Comparison of the results when the simulated annealing process was applied with objective function Ψ_1 .

Number of turbines	Objective function: $\Psi_1 = E_{TR}^s$ (MWh/year)					
	All combinations		Simulated Annealing (SA) solution			
	Recovered Energy (MWh)	Number of iterations	Recovered Energy (MWh)	Difference between SA and the best of all possible combinations (%)	Number of iterations to obtain optimized solution	Number of iterations done in the simulated annealing
2	10.16	190	10.16	0.00	1	792
3	11.63	1140	11.63	0.00	1	792
4	12.79	4845	12.79	0.00	54	792
5	13.81	15504	13.81	0.00	22	792
6	14.77	38760	14.77	0.00	86	792
7	15.60	77520	15.60	0.00	92	792
8	16.37	125970	16.37	0.00	38	792
9	17.00	167960	17.00	0.00	361	792
10	17.58	184756	17.58	0.00	73	792

Table 2
Comparison of the results when the simulated annealing process was applied with the objective function Ψ_2 .

Number of turbines	Objective function: $\Psi_2 = \frac{E_{TR}^s}{PSR}$ (MWh/year ²)					
	All combinations		Simulated Annealing (SA) solution			
	$\frac{E_{TR}^s}{PSR}$ (MWh/year ²)	Number of iterations	$\frac{E_{TR}^s}{PSR}$ (MWh/year ²)	Difference between SA and the best of all possible combinations (%)	Number of iterations to obtain optimized solution	Number of iterations done in the simulated annealing
2	3.77	190	3.77	0.00	1	594
3	4.15	1140	4.15	0.00	50	594
4	4.47	4845	4.47	0.00	13	594
5	4.46	15504	4.44	-0.37	42	594
6	4.44	38760	4.42	-0.30	132	594
7	4.44	77520	4.41	-0.48	428	594
8	4.46	125970	4.42	-0.82	169	594
9	4.50	167960	4.46	-0.94	165	594
10	4.53	184756	4.49	-1.01	214	594

connections to hydrants and irrigation points, and the remaining pipelines were secondaries and auxiliary lines. The number of modelled junctions were 646 elements. These were distributed on 341 consumption nodes, 70 elements were hydrants and the others were auxiliar nodes. The definition of the demand patterns were adopted according to the cited methodology in Section 2.4, in which, the demand depended on farmers' habit. The total number of developed patterns were 341 (one by each irrigation point), which were discretized by hourly intervals along a complete year.

4.3. Maximization of the theoretical energy recovered

According to the optimization methodology, this study used two different objective functions ($\Psi_1 = E_{TR}^s$ and $\Psi_2 = \frac{E_{TR}^s}{PSR}$). Previously, the ordered list of Ψ_1 and Ψ_2 must be generated. Table 3 shows the obtained values of the theoretical recovered energy, which were sorted in descendent order. The line with higher recovered energy was the line 38 with 90.28 MWh/year. The sorted lines according to Ψ_2 were developed considering the values of the recovered energy and the PSR, as well as the maximum theoretical power.

Once, the list was established, the maximization was carried out. Previously, a sensitivity analysis was performed to fix the different control parameters that were used to apply the simulated annealing algorithm. These values are shown in Table 4 for both objective functions.

Although Table 4 only showed a maximum of ten machines for each objective function, defining for each case the optimized solution, the methodology simulated the location of the 85 possible machines. Fig. 10 shows the obtained results for each objective function and the number of turbines. When Ψ_1 was analyzed, the maximum recovered energy was 83.79 MWh/year and this value was reached when 56 machines were simulated. However, the increase of the energy was lower than 8.34% between all simulations when a number above 10 machines was considered. The analysis of the second objective function (Ψ_2) showed a maximum baseline between 8 and 41 machines, in which the values were near 11.96 MWh/year². When the number of machines increased on 41 the objective function decreased.

Fig. 10 shows three different areas. Firstly, from zero to ten turbines, in which the function Ψ_2 improves when Ψ_1 grows. The

second area, from ten to forty-five turbines, in which both functions were constant, and the third zone, when the number of turbines was greater than forty-five, Ψ_2 got worse the function Ψ_1 was constant. Therefore, the significance area was the first one, in which, the both objective function had a similar behaviour, and the use of a multiobjective solution approach was not necessary because both functions are improved jointly by optimizing only one of them. The difference to the optimal solution when compared with the best obtained by analyzing all possible combinations is reduced (lower 1%). This small difference justifies the use of simulated annealing algorithms with much less computational effort. In the hypothesis where the objective functions are not correlated or the obtained results are not near the optimal solution, the use of the multiobjective metaheuristics algorithms, such as the particle swarm optimization (PSO) [5] will be recommendable.

When only one turbine is installed, the obtained result for both objective function was the same, and this line corresponded with the line 38. If the optimization is performed for two turbines, the solution in both objective function was also the same (lines 22 and 38). If a greater number than three turbines is considered, the solution depended on the analyzed objective function. However, in both cases, the lines 22 and 38 appeared, and these lines represented a recovered energy value above 78% (when Ψ_1 was maximized) and 85% if the maximized function is Ψ_2 . These results showed these lines were the main locations to recover energy. In all cases, the recovered energy was lower when the maximization is developed considering PSR value. The increment of the recovered energy oscillated between 1.10% (when four turbines were simulated) and 8.09% (when ten turbines were analyzed).

Finally, the selected objective function to model in WaterGEMS® in extended period simulation over time was the maximum recovered energy (Ψ_1) based on:

- a) Both solutions contained the main lines (22 and 38) and the line 5 when the solution with five turbines was analyzed.
- b) The PSR index was calculated from theoretical references, therefore, as the obtained results were similar, the recovered energy has been prioritized. In the case study, where the investment and maintenance costs are defined exactly based on market prices, the selection of lines by this objective function (ratio between E_{TR}^s and PSR) could be prioritized.

Table 3
Ordered list taking account the theoretical recovered energy in lines (E_T).

PIPE	E_T (MWh/year)	PIPE	E_T (MWh/year)	PIPE	E_T (MWh/year)	PIPE	E_T (MWh/year)
38	90.28	8	26.01	1	4.37	7	1.41
22	83.75	9	25.00	42	4.23	32	1.13
43	83.00	3	18.75	36	4.23	66	0.90
23	82.74	2	17.65	41	3.96	57	0.87
25	79.55	47	16.19	37	3.59	61	0.87
26	78.38	51	14.56	70	3.32	11	0.82
27	77.90	54	12.96	74	3.12	17	0.79
29	76.38	55	12.77	68	3.04	69	0.77
44	55.82	56	12.68	83	3.01	84	0.75
45	48.59	58	11.08	75	2.94	35	0.65
10	41.84	59	10.62	31	2.87	76	0.60
12	41.30	60	10.24	85	2.82	4	0.57
14	41.16	30	9.93	77	2.82	82	0.52
15	41.16	39	8.92	78	2.55	18	0.49
13	41.16	33	7.72	52	2.26	73	0.41
16	40.62	40	7.64	28	2.10	72	0.41
19	39.58	63	5.85	24	2.01	62	0.32
20	38.82	65	5.32	71	1.98	64	0.22
48	32.79	46	5.17	53	1.94	21	0.13
49	28.30	50	5.08	80	1.81	—	—
5	26.99	67	4.95	81	1.63	—	—
6	26.57	34	4.86	79	1.51	—	—

Table 4

Results of maximization according to the objective function.

OPTIMIZATION FOR THE MAXIMUM THEORETICAL E_{TR}^s												
$T_i = 100; T_f = 0.01; a = 0.9; L = 10$; Number of iterations = 7128												
n	LINES									E_{TR}^s (MWh/year)	PSR (year)	$\frac{E_{TR}^s}{PSR}$ (MWh/year ²)
1	38									49.66	5.46	9.10
2	22	38								60.36	5.65	10.68
3	22	38	59							66.20	5.99	11.05
4	22	38	47	59						69.00	6.31	10.94
5	5	22	38	47	59					71.25	6.22	11.45
6	5	22	38	47	58	59				73.25	6.28	11.67
7	5	22	38	47	58	59	70			74.44	6.41	11.61
8	5	22	38	39	47	58	59	70		75.34	6.53	11.54
9	2	10	22	39	43	47	58	59	70	75.92	6.79	11.19
10	2	10	22	39	43	47	58	59	70	76.80	6.85	11.21

OPTIMIZATION FOR THE RATIO BETWEEN E_{TR} AND PSR													
$T_i = 10; T_f = 0.01; a = 0.9; L = 10$; Number of iterations = 5346													
n	LINES									E_{TR}^s (MWh/year)	PSR (year)	$\frac{E_{TR}^s}{PSR}$ (MWh/year ²)	
1	38									49.66	5.46	9.10	
2	22	38								60.36	5.65	10.68	
3	5	22	38							62.61	5.58	11.23	
4	5	22	38	60						68.24	5.87	11.62	
5	5	22	38	56	60					69.68	5.96	11.69	
6	5	10	22	38	58	60				70.95	5.98	11.87	
7	5	10	22	27	38	58	60			70.95	5.98	11.87	
8	1	5	12	13	22	38	58	60		70.93	5.95	11.94	
9	1	5	10	22	38	48	58	54	60	71.05	5.95	11.95	
10	1	5	6	8	10	22	26	38	58	60	71.05	5.95	11.95

^a Averaged performance equal to 0.55 has been considered to determine the PSR index.

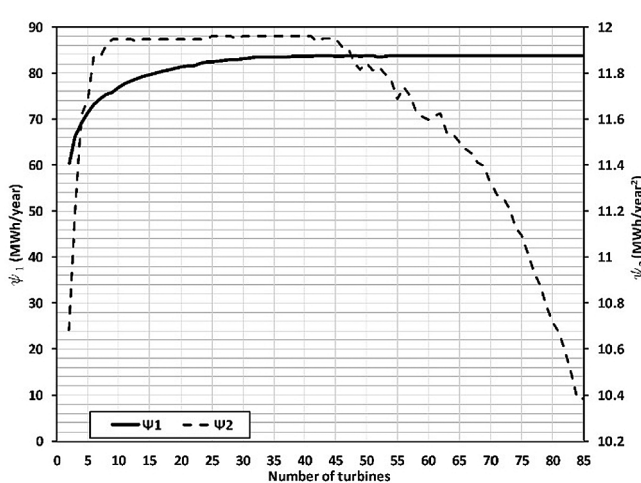


Fig. 10. Results of the proposed methodology for both objective functions (ψ_1 and ψ_2).

- c) The indexes of PSR were similar, and the option E_{TR}^s had more available energy to be recovered.
- d) This availability was verified in this network since in line 5, the points of the theoretical available head (H_T) were constant along the all flow range. When this uniformity occurred, the number of the necessary installed PATs will be very high to cover 80% of the operation range of flows at least. Hence, in line 5, the minimum number of machines was twelve and this high number is not convenient in any network due to the difficulty of the operation.
- e) Related to the cited points b) and d), if the location of the machines is optimized considering PSR index, the search of the vector in the simulated annealing must contain restrictions in the lines, in which the available machines cannot

operate independently. To do so, this objective function could be used when the economic parameters and the available machines will be exactly known.

- f) In this case study, when PSR index is considered in the optimization procedure, the obtained results were similar in many machines (5, 22, 38 and 58) that were located in the main branches of the network. Also, when different machines were allocated in series, the operation zone of upstream installed machines ($Q-H_T$) was very variable if this operation area is compared when there were no series installed machines. This phenomenon occurred because the demand's patterns were very variable over time in the irrigation network. Considering the optimization with E_{TR}^s , the location of the machines was more variable in terms of branch levels (*i.e.*, main, secondary, tertiary pipes).

The solution with four turbines (22 + 38+59 + 47 in Table 4) recovered 69.00 MWh/year. This solution represented 90% of the E_{TR}^s when ten turbines are optimized (76.80 MWh/year). In the following section, an energy analysis was developed in the network (Fig. 9) when the four assumptions were modelled on WaterGEMS®. The cases study were Case A (line 38); B (lines: 22 and 38); C (lines: 22, 38, and 59); and D (lines: 22, 38, 59, and 47).

4.4. Energy recovered with selected machines

4.4.1. Selection of PATs

PATs were selected with the described premises in Section 2.3: H_R cannot be greater than H_T to ensure the minimum service pressure, and the operation range must cover 80% of flow range at least. Also, the discharge and the head number were taken from Fig. 4. The characteristics of the selected machines are listed in Table 5. The specific speed of the selected PATs varied between 24.50 and 46.40 rpm and their fixed rotational speed were 2030 rpm (PATs simulated in line 59), 2500 rpm (PATs installed in line 38), and 2900 rpm (PAT in line 38 when this machine group

Table 5

Characteristics of selected PATs.

ASSUMPTION	A	B	C	D					
Characteristics of PAT	LINE ss (rpm) N (rpm) D (m) Q_{min} (l/s) Q_{max} (l/s) BEP- Q (l/s) BEP-H (m)	38 24.50 2900 0.14 5.88 16.98 13.24 43.22	22 24.50 2900 0.14 5.27 14.12 11.87 11.81	38 46.40 2500 0.10 5.12 15.03 10.58 8.52	59 39.40 2030 0.10 5.12 9.11 10.58 40.87	22 24.50 2900 0.14 5.27 14.12 10.58 11.81	38 46.40 2500 0.10 5.12 15.03 9.11 8.52	59 39.40 2030 0.10 5.12 14.12 10.58 11.81	47 35.30 2900 0.10 2.74 9.76 7.46 13.92
Values of PATs in Parallel	LINE n Q_{min} (l/s) Q_{max} (l/s) H_{Rmin} (m w.c.) H_{Rmax} (m w.c.) Range of operation of PATs (%) (MIN 80 %)	38 3 5.88 50.94 23.84 63.40 89.28	22 3 5.27 42.36 22.16 52.09 80.01	38 5.12 45.09 42.36 22.16 52.09 86.91	59 2.74 45.09 27.33 6.42 14.47 86.91	22 5.27 42.36 22.16 52.09 21.30	38 5.12 45.09 27.33 6.42 14.47 86.91	59 2.74 27.33 10.09 3.98 14.47 85.10	47 3.22 27.20 10.09 3.98 27.50 99.91
Theoretical Values In Line	LINE H_{Tmax} (m w.c.) Q_{min} (l/s) Q_{max} (l/s)	38 79.40 0.18 106.00	22 56.35 0.19 137.27	38 56.35 0.18 106.00	59 24.12 0.19 137.27	22 18.60 0.23 106.00	38 56.35 0.19 137.27	59 24.12 0.23 106.00	47 18.60 0.70 76.07
									41.76

operated alone as well as the *PATs* in line 22). The fixed rotational speed was constant in any time and was defined to adjust the recovered head to the theoretical available head.

The selected machines described in Table 5, ensured the minimum pressure in all consumption nodes and over time. Also, *PATs* can operate upper to 80% of the flow, reaching 99.91% in line 47. In lines 38 and 59 the operation range was above 85%.

The values of the discharge and the head number as well as the performance of these turbines were used to select the more appropriate machine, according to the available head in each case. The efficiency values were used supposing the affinity laws in the recovery machines. However, the use of variable efficiency as a function of the discharge number is more realistic and it can help to define the weighted average efficiency of these machines when the flow variability is significance.

4.4.2. Recovered energy

Tables 6 and 7 contain the obtained results by using WaterGEMS®. Table 6 describes the characteristic of the operation values in each installed *PAT*, depending on the line and the assumption. The maximum developed power (7.83 kW) occurred when *PATs* were only installed in line 38. This scenario presented the highest power values in each machine. The recovered energy can be visualized in Table 6 by each simulated *PAT*, as well as its operation time along the year and its performance (*i.e.*, maximum, minimum and weighted efficiency) in each case.

The results in Table 7 refer to the energy recovery in each simulated line and global in the network. The maximum recovered energy in a line was obtained when the case A was considered (25.41 MWh/year). If this value is compared to the theoretical recovered energy (E_{TR}) in the same scenario, the recovery coefficient (RC) was 0.28. Therefore, in this case, 28% of the available energy can be recovered and the weighted average efficiency was 68.46%.

Fig. 11 (A and B) shows the operation zone in the line 38, when a *PAT* was installed in series in the line 22. The theoretical available head in line 38 varied substantially, as Fig. 11 illustrates, when *PATs* were installed or not in line 22. If *PATs* are connected in series, the points of the operation zone were more dispersed when the same line was compared with no series installed machines. This spread of the theoretical work points caused the reduction of the operation time, which is showed in Table 6. However, the weighted performance was similar because the selected machines were different in

each simulated assumption, because the aims was to maximize the recovered energy as a function of the theoretical available head.

The assumption A and B were again simulated, assuming that the installed machines in line 38 were the same with the objective to analyze the caused effect by the installation of the *PATs* in series, RC was 0.09 in line 38 when *PATs* in line 22 didn't operate. If Fig. 11 (B) is observed, the available head varied between 23 and 80 m w.c. when the machines were installed in series (for the operation range from 5.12 to 45.09 l/s). However, the majority of the recovery points were between 23 and 59 m w.c.. When the energy was only recovered in line 38, H_T oscillated between 70 and 80 m w.c. for the same operation flow range.

Fig. 11 (C) shows the pressure in node 32 (this junction simulated a hydrant, as shown in Fig. 11 (D)). In this node, the pressure value was reduced when the turbines were in operation. The pressure in the hydrant varied from 85 m w.c. (for *PATs* not operation) to 40 m w.c. (when *PATs* was in operation). Also, this figure shows the total recovered energy over time when the four groups of the *PATs* were operating, as well as the instant efficiency of the installed *PAT* in line 38. For this recovery system, the obtained efficiency values were near 75%. Similar information can be obtained in all nodes, lines and installed machines when applying the described methodology.

Fig. 12 shows the different operation points of the recovered head and the efficiency in each *PAT*. These points were obtained with WaterGEMS®. This figure shows when there was a short flow interval, the *PAT* efficiency was high (*e.g.*, in line 47, the maximum efficiency was 84% and it was above 70% in all operation range, which was between 4.2 and 8.2 l/s). However, other *PATs* with greater operation range of the flows, the efficiency varied between 15 and 75% and the flow range between 5 and 15 l/s, approximately.

Table 7 allows modelers to determine the operation time and the recovered energy of each *PAT*. If the total recovered energy in the network is analyzed, the highest recovery energy was obtained when the assumption D was simulated, considering four groups of turbines operated along the year. In this case, the recovered energy was 30.52 MWh/year and the total recovery coefficient (TRC) in the network was 0.24. However, if this value is compared with the case A (25.41 MWh/year, in Table 7), the increase of the recovered energy was 5.11 MWh (20.11%), but the necessary installed power varied from 23.42 to 30.11 kW (an increase of 28.56%). If the analysis is performed with the theoretical recovered energy, the increase of the E_{TR} was 38.76%. This value showed the increase of the

Table 6

Balance of the recovered energy in each PAT.

ASSUMPTION	LINE	BALANCE IN EACH PAT							VARIABLE	OPERATION			
		Q _{max} (l/s)	Q _{min} (l/s)	P _{max} (kW)	P _{min} (kW)	h _{max} (%)	h _{min} (%)	h _w (%)		NO PAT	PAT1	PAT2	PAT3
A	38	16.99	6.05	7.83	0.27	74.15	19.29	68.46	t (h)	4566	4194	2020	565
B	22	14.00	5.01	5.34	0.11	74.58	9.86	65.85	E _R (MWh/year)	—	10.29	3.53	0.91
	38	15.00	5.00	2.21	0.04	74.95	11.77	71.85	% E _R	—	69.85	23.99	6.16
C	22	14.00	5.01	5.34	0.11	74.58	9.86	65.85	t (h)	4600	4160	2191	619
	38	15.00	5.00	2.21	0.04	74.95	11.77	71.85	E _R (MWh/year)	—	6.48	2.42	0.91
	59	9.00	3.03	0.97	0.02	81.06	15.35	75.78	% E _R	—	66.07	24.67	9.26
D	22	14.00	5.01	5.34	0.11	74.58	9.86	65.85	t (h)	4600	4160	2191	619
	38	15.00	5.00	2.21	0.04	74.95	11.77	71.85	E _R (MWh/year)	—	6.48	2.42	0.91
	59	9.00	3.03	0.97	0.02	81.06	15.35	75.78	% E _R	—	66.07	24.67	9.26
	47	8.99	4.41	1.92	0.34	84.90	69.64	82.53	t (h)	5846	2914	1415	534
									E _R (MWh/year)	—	0.81	0.32	0.11
									% E _R	—	65.37	25.55	9.08
									t (h)	6931	1319	461	49
									E _R (MWh/year)	—	0.96	0.43	0.07
									% E _R	—	66.01	29.32	4.67

Table 7

Balance of the recovered energy in each line and the global in the network.

ASSUMPTION	LINE	BALANCE IN THE LINE							BALANCE IN THE NETWORK					
		P _{max} (kW)	VARIABLE	OPERATION			E _R (MWh/year)	E _{TR} (MWh/year)	RC	P _{max} (kW)	E _R (MWh/year)	E _{TR} (MWh/year)	TRC	
				PAT STOP	1PAT	2PATs								
A	38	23.42	t (h)	4566	2174	1455	565	25.41	90.29	0.28	23.42	25.41	90.28	
			E _R (MWh/year)	—	6.75	5.25	2.72						0.28	
			% E _R	—	45.86	35.65	18.49							
B	22	16.00	t (h)	4600	1969	1572	619	18.29	83.75	0.22	22.60	26.18	109.75	
			E _R (MWh/year)	—	4.06	3.03	2.73						0.24	
	38	6.60	t (h)	4600	1969	1572	619	7.89	26.00	0.30				
			E _R (MWh/year)	—	1.88	1.71	0.87							
			% E _R	—	42.13	38.33	19.54							
C	22	16.00	t (h)	4600	1969	1572	619	18.29	83.75	0.22	25.50	28.50	120.37	
			E _R (MWh/year)	—	4.06	3.03	2.71						0.24	
	38	6.60	t (h)	4600	1969	1572	619	7.89	26.00	0.30				
			E _R (MWh/year)	—	1.88	1.71	0.87							
			% E _R	—	42.13	38.33	19.54							
	59	2.90	t (h)	5846	1499	881	534	2.32	10.62	0.22				
			E _R (MWh/year)	—	0.49	0.41	0.34							
			% E _R	—	39.82	32.95	27.23							
D	22	16.00	t (h)	4600	1969	1572	619	18.29	83.75	0.22	31.00	30.52	125.46	
			E _R (MWh/year)	—	4.06	3.03	2.71						0.24	
	38	6.60	t (h)	4600	1969	1572	619	7.89	26.00	0.30				
			E _R (MWh/year)	—	1.88	1.71	0.87							
			% E _R	—	42.13	38.33	19.54							
	59	2.90	t (h)	5846	1499	881	534	2.32	10.62	0.22				
			E _R (MWh/year)	—	0.49	0.41	0.34							
			% E _R	—	39.82	32.95	27.23							
	47	5.49	t (h)	6931	1829	510	49	2.02	5.09	0.40				
			E _R (MWh/year)	—	1.20	0.24	0.02							
			% E _R	—	82.23	16.21	1.56							

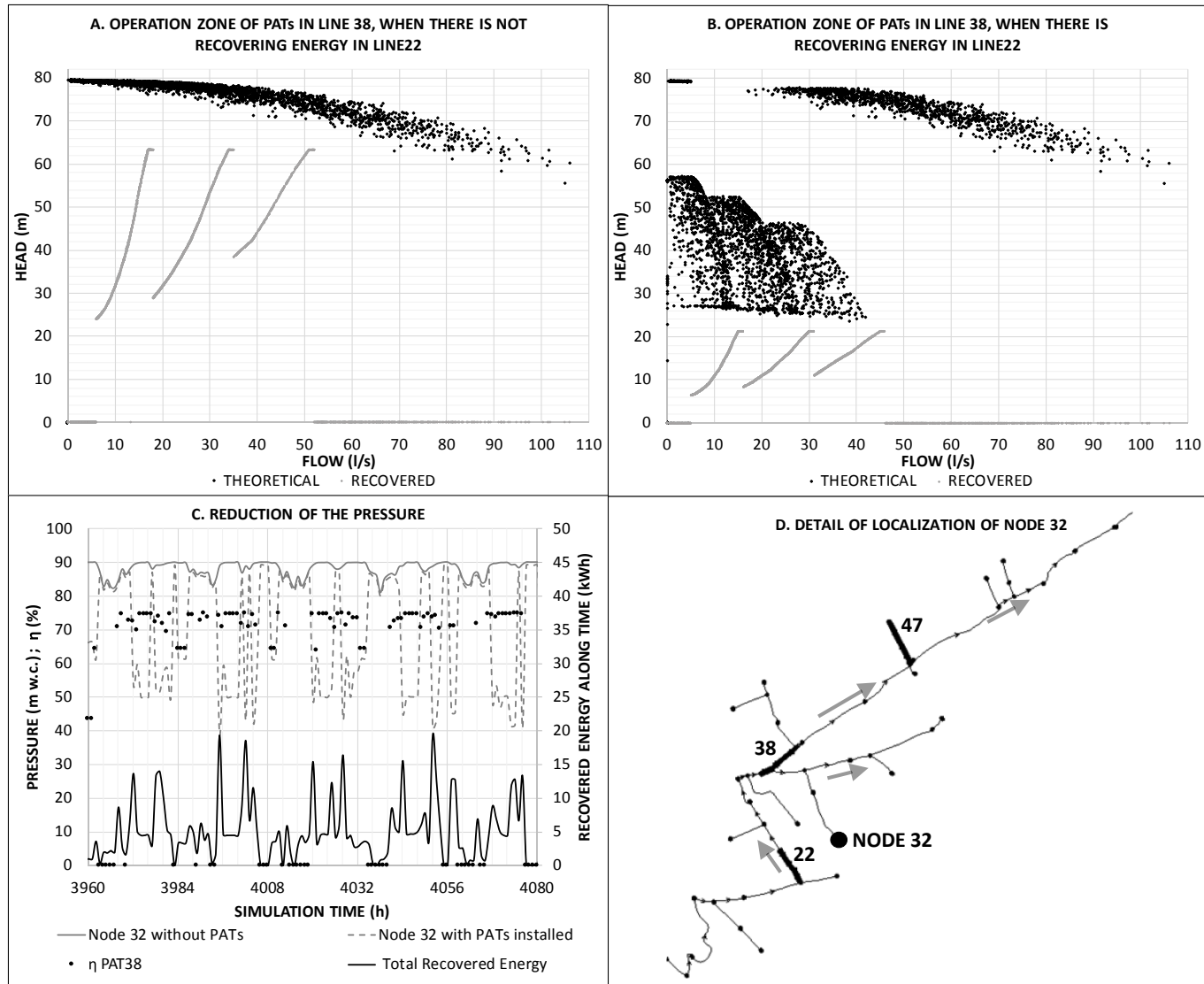


Fig. 11. Variation of H_T with PATs installed in series.

number of the installed PATs in different lines reduced the TRC values in the network. Fig. 13 shows these results, in which E_{TR} and E_R were represented. In this figure, the recovered energy trend can be observed in both cases (theoretical and recovered) and it summarized the values in Table 7. This figure represents the increase of the recovered energy was smaller than the theoretical recovered energy, when the number of analyzed lines with installed recovery systems grew. If the recovered energy is compared considering the feasibility indexes, the case B presented the best economic indicators ($PSR = 5.47$ and $EI = 0.47$) and both indexes were below 6 and 0.6, respectively. All studied cases were feasible, except assumption D, in which, the presented PSR value was 6.44. Fig. 13 also shows that the variation between theoretical and recovered indexes was not important. Theoretical and recovered PSR values varied between 5.5 and 6.5 (theoretical values: Case A = 5.46; B = 5.65; C = 5.58; and D = 5.87; recovered values: A = 5.85; B = 5.48; C = 5.68; and D = 6.44). This difference was due to the variation of the efficiency over time when the turbined flow changed.

The case A was reconsidered again (so-called 'Case A*' in Fig. 13) with variable rotational speed in PAT1 that previously had fixed

rotational speed (n_0) equal to 2900 rpm, keeping its specific speed (ss) and diameter of the impeller.

Hence, the rotational speed of the PAT1 varied in the following ranges: a) 1450 rpm ($\alpha = \frac{n}{n_0} = 0.5$) for the flow between 2.94 l/s and 5 l/s; b) 2320 rpm ($\alpha = 0.8$) for the flow between 5 and 9 l/s; 2900 rpm ($\alpha = 1.0$) between 9 and 14 l/s; and c) 3480 rpm ($\alpha = 1.2$) for the flow between 14 and 18.5 l/s. For this situation, when the flow were above 18.5 l/s, the recovery systems (PAT1, PAT2, and PAT3) operated with the same rotational speed (2900 rpm) to ensure the minimum pressure as well as the machines recovered the same head. In this case, the recovered energy was 26.52 MWh/year. This value was 4.33% higher than the case A (25.41 MWh/year in Table 7). Also, the use of variable speed in line 38 recovered more energy than in the case B, which was integrated by two groups of PATs in parallel. In this case, the existence of a single group of installed machines makes possible the improvement of the water management of the network as well as the reduction of maintenance costs.

Finally, when the annual energy balance was performed, considering the solution of the 'Case A*', the energy was distributed in the followings terms: 4.10% was dissipated by friction, 27.45%

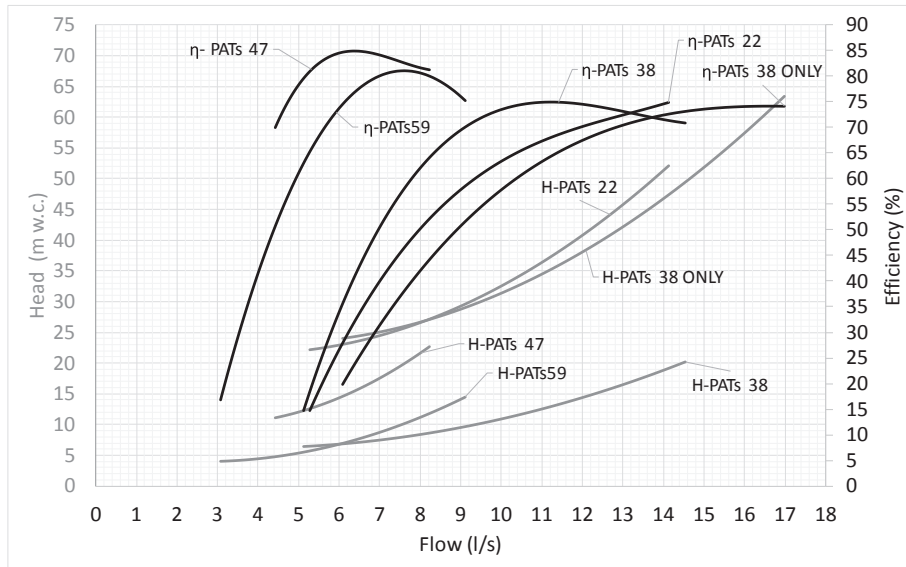


Fig. 12. Head (H_R) and performance (η) obtained with WaterGEMS® depending on PAT installed.

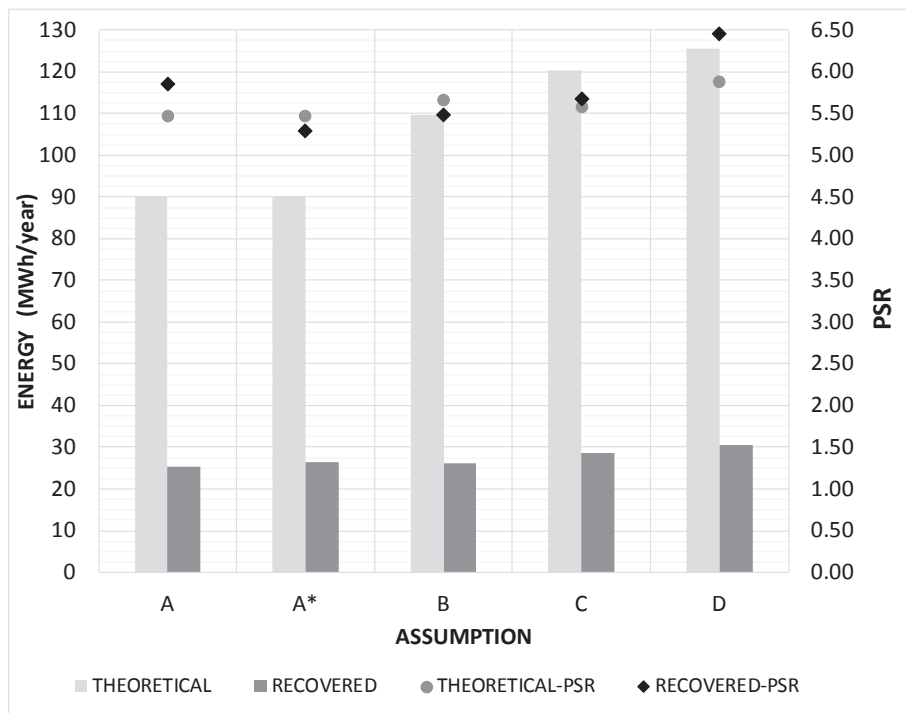


Fig. 13. E_{TR} , E_R , PSR, and EI as a function of the cases.

was necessary to ensure the irrigation service, 58.90% was non-recoverable with the proposed solution (i.e., only one group of machines installed with variable rotational speed), and 9.55% of the provided energy can be recovered when the machines were installed in line 38. This value of recovered energy was obtained, when the annual consumed volume in the network was 927553 m³. This recovered energy supposed an average recovery index equal to 0.03 kWh/m³.

5. Conclusions

This research showed the energy recovery in agricultural water

networks is a technologically feasible alternative to improve the energy efficiency of these systems, as a sustainability alternative to be used in self-consumption or sale. On the one hand, an optimization methodology to maximize the recovered energy were proposed by using simulated annealing algorithm. Although there are other heuristic techniques such as tabu search or genetic algorithms, which can also contribute to solve the problem, the simulated annealing showed good performance when the calculus time and the final solution were analyzed both synthetic network and real case study considering the constrained conditions. Then, although different authors developed comparisons between heuristic techniques, is difficult to select the best technique because it

depends on particular constrained conditions [29,49]. In the comparisons developed, tabu search and simulated annealing showed better results with major frequency than genetic algorithms. Therefore, the selection of the location problems is not established in advance. In this sense, the use of the simulated annealing optimization techniques to allocate control elements or turbines is a suitable choice [47,49], while the application of the particle swarm optimization is successfully applied in the cost analysis when hybrid renewable generation (wind and photovoltaic) was analyzed [5].

As novelty, the recovered energy maximization was proposed through objective functions for the ratio between maximum recovered energy and the feasibility index, particularly the period simple return, optimizing the water system using the simulated annealing algorithm as the water management tool. When these results were compared with the obtained values when the considered objective function of the maximum recovered energy, the total recovered energy and PSR were similar. However, the use of the PSR in the maximization can be introduced when the water management get the market prices as well as the characteristic curves of the available machines. If the manager knows these parameters, objective criteria in the simulated annealing to discriminate the lines can be established where the installation of the recovery systems is not possible and the solution of the maximization will avoid incorrect solutions.

On the other hand, the analysis of the real case study determined when the machines were installed in series in the main lines, the operation zone was modified due to the upstream machine. This variation of the operation zone by the dispersion of the data pairs (Q,H) caused the decrease of the operation time and the recovered energy because there were more operation points which were not inside of operation range of the hydraulic machine. Therefore, a possible criterion to discriminate the maximization is to avoid machines installed in the same branch's levels to avoid the dispersion of the operation points.

The analyzed cases in this research presented TRC values between 0.28 and 0.24. This TRC value decreased, as the number of turbines increased. Case B was the solution more viable when the rotational speed was considered fixed. However, if the rotational speed is variable (Case A*), more energy was recovered. If the same assumption A is compared (with/without variable speed), the recovered energy increased 4.33% with variable speed. When the energy balance in the network was performed, 9.55% of the provided energy to the network can be recovered while the dissipated energy by friction represented 4.10% in the balance. Therefore, Case A \times of one group with three turbines in parallel was the more viable solution and the recovered energy was maximum, being up to 26.51 MW h/year and the PSR was minimum, down to 5.28.

Finally, the use of this proposed methodology allows water managers to improve the water distribution networks by using simulated annealing optimization as a helpful tool, ensuring the quality of the service all the time, searching for the sustainability in irrigation networks through the maximization of the recovered energy, and increasing the energy efficiency in water systems.

Acknowledgments

This research is supported by Program to support the academic career of the faculty of the Universitat Politècnica de València 2015/2016 in the project “Methodology for Analysis of Improvement of Energy Efficiency in Irrigation Pressurized Network”. The authors also thank PhD. Díaz-Madroñero by contributing to improve the contents of this manuscript related to the optimization; and Bentley Systems for availability of WaterGEMS software through

IST licenses.

References

- [1] R. Abadia, M.C. Rocamora, J.I. Corcoles, A. Ruiz-Canales, A. Martínez-Romero, M.A. Moreno, Comparative analysis of energy efficiency in water users associations, Span. J. Agric. Res. 8 (2010) 134, <https://doi.org/10.5424/sjar/201008S2-1356>.
- [2] L.S. Araujo, H. Ramos, S.T. Coelho, Pressure control for leakage minimisation in water distribution systems management, Water Resour. Manag. 20 (2006) 133–149, <https://doi.org/10.1007/s11269-006-4635-3>.
- [3] M. Arriga, Pump as turbine – a pico-hydro alternative in Iao People's democratic republic, Renew. Energy 35 (2010) 1109–1115, <https://doi.org/10.1016/j.renene.2009.08.022>.
- [4] H. Baghaee, M. Mirsalim, G. Gharehpetian, A. Kaviani, Security/cost-based optimal allocation of multi-type FACTS device using particle swarm optimization, Simulation 88 (2012) 999–1010, <https://doi.org/10.1177/0031549712438715>.
- [5] H.R. Baghaee, M. Mirsalim, G.B. Gharehpetian, H.A. Talebi, Reliability/cost-based multi-objective Pareto optimal design of stand-alone wind/PV/FC generation microgrid system, Energy 115 (2016) 1022–1041, <https://doi.org/10.1016/j.energy.2016.09.007>.
- [6] H.R. Baghaee, M. Mirsalim, G.B. Gharehpetian, Multi-objective optimal power management and sizing of a reliable wind/PV microgrid with hydrogen energy storage using MOPSO, J. Int. Fuzzy Syst. 32 (2017) 1753–1773, <https://doi.org/10.3233/JIFS-152372>.
- [7] E. Cabrera, R. Cobacho, J. Soriano, Towards an energy labelling of pressurized water networks, Procedia Eng. 70 (2014) 209–217, <https://doi.org/10.1016/j.proeng.2014.02.024>.
- [8] J. Cabrera, Calibración de Modelos Hidrológicos [WWW Document], Imefen.Uni.Edu.Pe, 2009. http://www.imefen.un.edu.pe/Temas_interes/modhidro_2.pdf.
- [9] A. Carravetta, G. Del Giudice, O. Fecarotta, H. Ramos, Energy production in water distribution networks: a PAT design strategy, Water Resour. Manag. 26 (2012) 3947–3959, <https://doi.org/10.1007/s11269-012-0114-1>.
- [10] A. Carravetta, G. Del Giudice, O. Fecarotta, H. Ramos, PAT design strategy for energy recovery in water distribution networks by electrical regulation, Energies 6 (2013a) 411–424, <https://doi.org/10.3390/en6010411>.
- [11] A. Carravetta, G. Del Giudice, O. Fecarotta, H. Ramos, Pump as turbine (PAT) design in water distribution network by system effectiveness, Water 5 (2013b) 1211–1225, <https://doi.org/10.3390/w5031211>.
- [12] A. Carravetta, O. Fecarotta, G. Del Giudice, H. Ramos, Energy recovery in water systems by PATs: a comparisons among the different installation schemes, Procedia Eng. 70 (2014) 275–284, <https://doi.org/10.1016/j.proeng.2014.02.031>.
- [13] A. Castro, Minicentrales Hidroeléctricas, Instituto para la Diversificación y Ahorro de la Energía, Madrid, 2006.
- [14] J. Chen, H.X. Yang, C.P. Liu, C.H. Lau, M. Lo, A novel vertical axis water turbine for power generation from water pipelines, Energy 54 (2013) 184–193, <https://doi.org/10.1016/j.energy.2013.01.064>.
- [15] A. Choulot, Energy recovery in existing infrastructures with small hydropower plants, FP6 Project Shapes (work package 5–WP5), European Directorate for Transport and Energy, 2010.
- [16] M. Conceição Cunha, L. Ribeiro, Tabu search algorithms for water network optimization, Eur. J. Oper. Res. 157 (2004) 746–758, [https://doi.org/10.1016/S0377-2217\(03\)00242-X](https://doi.org/10.1016/S0377-2217(03)00242-X).
- [17] L. Corcoran, D. Ph, A. McNabola, D. Ph, P. Coughlan, D. Ph, Optimization of water distribution networks for combined hydropower energy recovery and leakage reduction, J. Water Resour. Plan. Manag. 142 (2015) 1–8, [https://doi.org/10.1061/\(ASCE\)WR.1943-5452.0000566](https://doi.org/10.1061/(ASCE)WR.1943-5452.0000566).
- [18] S. Derakhshan, A. Nourbakhsh, Experimental study of characteristic curves of centrifugal pumps working as turbines in different specific speeds, Exp. Therm. Fluid Sci. 32 (2008) 800–807, <https://doi.org/10.1016/j.expthermflusci.2007.10.004>.
- [19] F. Estrada, H. Ramos, Micro-hydro solutions in Alqueva Multipurpose Project (AMP) towards water-energy-environmental efficiency improvements, Dissertation Project at IST, ESCOLA TÉCNICA SUPERIOR D'ENGINYERIA INDUSTRIAL DE BARCELONA, 2015.
- [20] M. Giugni, N. Fontana, A. Ranucci, Optimal location of PRVs and turbines in water distribution systems, J. Water Resour. Plan. Manag. 140 (2014) 06014004, [https://doi.org/10.1061/\(ASCE\)WR.1943-5452.0000418](https://doi.org/10.1061/(ASCE)WR.1943-5452.0000418).
- [21] J.A. Imbernon, B. Usquín, Sistemas de generación hidráulica. Una Nueva Forma Entender la Energ, in: II Congreso Smart Grid, 2014.
- [22] M.A. Jiménez-Bello, A. Royuela, J. Manzano, A.G. Prats, F. Martínez-Alzamora, Methodology to improve water and energy use by proper irrigation scheduling in pressurised networks, Agric. Water Manag. 149 (2015) 91–101, <https://doi.org/10.1016/j.agwat.2014.10.026>.
- [23] A. Kaviani, H. Baghaee, G. Riahy, Optimal Sizing of a stand-alone wind/photovoltaic generation unit using particle swarm optimization, Simulation 85 (2009) 89–99.
- [24] S. Kirkpatrick, C. Gelatt, M. Vecchi, Optimization by simulated annealing, Science 220 (1983) 671–680 (80–).
- [25] I. Kougas, T. Patsialis, A. Zafirakou, N. Theodossiou, Exploring the potential of energy recovery using micro hydropower systems in water supply systems,

- Water Util. J.** 7 (2014) 25–33.
- [26] S.-F. Kuo, C.-W. Liu, S.-K. Chen, Comparative study of optimization techniques for irrigation project planning, *J. Am. Water Resour. Assoc.* 39 (2003) 59–73, <https://doi.org/10.1111/j.1752-1688.2003.tb01561.x>.
- [27] S. Malavasi, G. Ferrarese, M.M.A. Rossi, A control valve for energy harvesting, *Procedia Eng.* 89 (2014) 588–594, <https://doi.org/10.1016/j.proeng.2014.11.482>.
- [28] S. Malavasi, M.M.A. Rossi, G. Ferrarese, GreenValve: hydrodynamics and applications of the control valve for energy harvesting, *Urban Water J.* (2016), <https://doi.org/10.1080/1573062X.2016.1175483>, 9006, Accepted paper.
- [29] A. Marvin, K. Sukran, K. Basheer, An empirical comparison of tabu search, simulated annealing, and genetic algorithms for facilities location problems, *Int. J. Prod. Econ.* 103 (2006) 742–754, <https://doi.org/10.1016/j.ijpe.2005.08.010>.
- [30] C. Mataix, *Turbomáquinas Hidráulicas*, Universidad Pontificia Comillas, Madrid, 2009.
- [31] N. Metropolis, A. Rosenbluth, M. Rosenbluth, A. Teller, E. Teller, Simulated annealing, *J. Chem. Phys.* 21 (1953) 1087–1092.
- [32] M. Moreno, J. Córcoles, J. Tarjuelo, J. Ortega, Energy efficiency of pressurised irrigation networks managed on-demand and under a rotation schedule, *Biosyst. Eng.* 107 (2010) 349–363, <https://doi.org/10.1016/j.biosystemseng.2010.09.009>.
- [33] D.N. Moriasi, J.G. Arnold, M.W. Van Liew, R.L. Binger, R.D. Harmel, T.L. Veith, Model evaluation guidelines for systematic quantification of accuracy in watershed simulations, *Trans. ASABE* 50 (2007) 885–900, <https://doi.org/10.13031/2013.23153>.
- [34] A. Nazari, H. Meisami, *Instructing WaterGEMS Software Usage*, 2008 (Tehran).
- [35] M. Nogueira, J. Perrella, Energy and hydraulic efficiency in conventional water supply systems, *Renew. Sustain. Energy Rev.* 30 (2014) 701–714, <https://doi.org/10.1016/j.rser.2013.11.024>.
- [36] M.A. Pardo, J. Manzano, E. Cabrera, J. García-Serra, Energy audit of irrigation networks, *Biosyst. Eng.* 115 (2013) 89–101, <https://doi.org/10.1016/j.biosystemseng.2013.02.005>.
- [37] M. Pérez-Sánchez, F. Sánchez-Romero, H. Ramos, P. López-Jiménez, Modeling irrigation networks for the quantification of potential energy recovering: a case study, *Water* 8 (2016) 1–26, <https://doi.org/10.3390/w8060234>.
- [38] M. Pérez-Sánchez, F. Sánchez-Romero, H. Ramos, P. López-Jiménez, Energy recovery in existing water networks: towards greater sustainability, *Water* 9 (2017) 97, <https://doi.org/10.3390/w9020097>.
- [39] A.G. Prats, S.G. Picó, F.M. Alzamora, M.Á.J. Bello, Random Scenarios Generation with Minimum Energy Consumption Model for Sectoring Optimization in Pressurized Irrigation Networks Using a Simulated Annealing Approach, 2011, [https://doi.org/10.1061/\(ASCE\)IR.1943-4774.0000452](https://doi.org/10.1061/(ASCE)IR.1943-4774.0000452).
- [40] H. Ramos, A. Borga, Pumps as turbines: an unconventional solution to energy production, *Urban Water* 1 (1999) 261–263, [https://doi.org/10.1016/S1462-0758\(00\)00016-9](https://doi.org/10.1016/S1462-0758(00)00016-9).
- [41] H.M. Ramos, A. Borga, M. Simão, New design solutions for low-power energy production in water pipe systems, *Water Sci. Eng.* 2 (2009) 69–84, <https://doi.org/10.3882/j.issn.1674-2370.2009.04.007>.
- [42] H. Ramos, M. Mello, P.K. De, Clean power in water supply systems as a sustainable solution: from planning to practical implementation, *Water Sci. Technol. Water Supply* 10 (2010) 39–49, <https://doi.org/10.2166/ws.2010.720>.
- [43] S. Rawal, J. Kshirsagar, Simulation on a pump operating in a turbine mode, in: *Proceedings of the 23rd International Pump Users Symposium*, Texas A & M University, Houston, 2007, pp. 21–27.
- [44] J. Reca, J. Martínez, C. Gil, R. Baños, Application of several meta-heuristic techniques to the optimization of real looped water distribution networks, *Water Resour. Manag.* 22 (2008) 1367–1379, <https://doi.org/10.1007/s11269-007-9230-8>.
- [45] J.A. Rodriguez-Díaz, E. Camacho-Poyato, M.T. Carrillo-Cobo, The role of energy audits in irrigated areas. The case of “Fuente Palmera” irrigation district (Spain), *Span. J. Agric. Res.* (2010).
- [46] R.A. Rutenbar, Simulated annealing algorithms: an overview, *IEEE Circuits Devices Mag.* 5 (1989) 19–26, <https://doi.org/10.1109/101.17235>.
- [47] I. Samora, M. Franca, A. Schleiss, H. Ramos, Simulated annealing in optimization of energy production in a water supply network, *Water Resour. Manag.* 30 (2016a) 1533–1547, <https://doi.org/10.1007/s11269-016-1238-5>.
- [48] I. Samora, V. Hasmatuchi, C. Münch-Aligné, M.J. Franca, A.J. Schleiss, H.M. Ramos, Experimental characterization of a five blade tubular propeller turbine for pipe inline installation, *Renew. Energy* 95 (2016b) 356–366, <https://doi.org/10.1016/j.renene.2016.04.023>.
- [49] M. Sinclair, Comparison of the performance of modern heuristics for combinatorial optimization on real data, *Comput. Oper. Res.* 20 (1993) 687–695.
- [50] P. Singh, Optimization of the Internal Hydraulic and of System Design in Pumps as Turbines with Field Implementation and Evaluation, University of Karlsruhe, 2005.
- [51] J. Tospronsampa, I. Kita, M. Ishii, Y. Kitamura, Split-pipe design of water distribution network using simulated annealing, *World Acad. Sci. Eng. Technol. Int. J. Environ. Chem. Ecol. Geol. Geophys. Eng.* 1 (2007) 28–38.
- [52] P.J.M. van Laarhoven, E.H.L. Aarts, Simulated annealing, in: *Simulated Annealing: Theory and Applications*, Springer Netherlands, Dordrecht, 1987, pp. 7–15, <https://doi.org/10.1007/978-94-015-7744-1>.
- [53] J.L. Verdegay, R.R. Yager, P.P. Bonissone, On heuristics as a fundamental constituent of soft computing, *Fuzzy Sets Syst.* 159 (2008) 846–855, <https://doi.org/10.1016/j.fss.2007.08.014>.
- [54] S.S. Yang, S. Derakhshan, F.Y. Kong, Theoretical, numerical and experimental prediction of pump as turbine performance, *Renew. Energy* 48 (2012) 507–513, <https://doi.org/10.1016/j.renene.2012.06.002>.
- [55] H. Youssef, M. Sait, H. Adiche, Evolutionary algorithms, simulated annealing and tabu search: comparative study, *Eng. Appl. Artif. Intell.* 14 (2001) 167–181, [https://doi.org/10.1016/S0952-1976\(00\)00065-8](https://doi.org/10.1016/S0952-1976(00)00065-8).
- [56] D.A. Zema, A. Nicotra, V. Tamburino, S.M. Zimbone, A simple method to evaluate the technical and economic feasibility of micro hydro power plants in existing irrigation systems, *Renew. Energy* 85 (2016) 498–506, <https://doi.org/10.1016/j.renene.2015.06.066>.